In situ evidence of magnetic reconnection in turbulent plasma

A. RETINÒ[1,2]*, D. SUNDKVIST[3], A. VAIVADS[1], F. MOZER[3], M. ANDRÉ[1] AND C. J. OWEN[4]

[1]Swedish Institute of Space Physics, SE-75121 Uppsala, Sweden
[2]Department of Astronomy and Space Physics, Uppsala University, SE-75120 Uppsala, Sweden
[3]Space Sciences Laboratory, University of California, Berkeley, California 94720, USA
[4]Mullard Space Science Laboratory, University College London, Dorking, RH5 6NT, UK
*e-mail: Alessandro.Retino@irfu.se

Magnetic reconnection is a universal process leading to energy conversion in plasmas[1]. It occurs in the Solar System[2–7], in laboratory plasmas[8] and is important in astrophysics[9,10]. Reconnection has been observed so far only at large-scale boundaries between different plasma environments[4–8]. It is not known whether reconnection occurs and is important in turbulent plasmas where many small-scale boundaries can form. Solar[11] and laboratory[12] measurements as well as numerical simulations[13–16] indicate such possibility. Here we report, for the first time, *in situ* evidence of reconnection in a turbulent plasma. The turbulent environment is the solar wind downstream of the Earth's bow shock. We show that reconnection is fast and electromagnetic energy is converted into heating and acceleration of particles. This has significant implications for laboratory and astrophysical plasmas where both turbulence and reconnection should be common.

The Earth's bow shock forms owing to the interaction of the Earth's magnetosphere with the solar-wind flow[17]. The region downstream of the bow shock, the magnetosheath, is one of the most turbulent environments in the near-Earth space. The turbulence is stronger when the magnetic field in the solar wind is directed approximately along the shock normal, the so-called quasi-parallel shock[18]. Downstream of the quasi-parallel shock, large-amplitude fluctuations in density and magnetic field have been observed[18] and thin current sheets are likely to form. Magnetic reconnection is easily initiated in thin current sheets[19]. Therefore, the magnetosheath is an ideal laboratory to study *in situ* magnetic reconnection in a turbulent plasma. Here we present, for the first time, *in situ* evidence of magnetic reconnection in a turbulent plasma using spacecraft observations in a thin current sheet found in the magnetosheath downstream of the quasi-parallel shock. We show that reconnection is important for heating and acceleration of particles in turbulent plasma.

We analyse four Cluster spacecraft[20] data from 27 March 2002. Figure 1a shows the spacecraft orbit. The spacecraft separation for this event is about 100 km. Figure 1b shows a schematic diagram of how thin current sheets could be formed in the turbulent plasma downstream of the quasi-parallel shock, together with a schematic diagram of magnetic reconnection. Figure 2 shows an overview of plasma and magnetic-field observations. The spacecraft cross the bow shock around 09:35 universal time. Between 09:35 and 11:00, the spacecraft are in the magnetosheath downstream of the quasi-parallel shock, the angle between the interplanetary
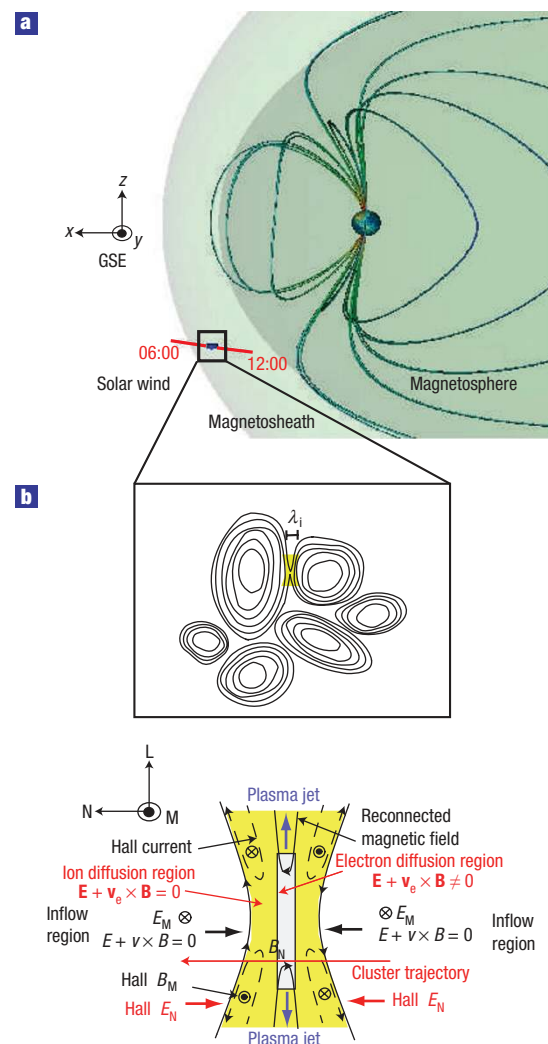
Figure 1 The quasi-parallel bow-shock crossing. a, Spacecraft orbit (red line). **b**, Schematic diagram of the current-sheet formation between magnetic islands and of magnetic reconnection in the current sheet. GSE: geocentric solar ecliptic coordinate system.
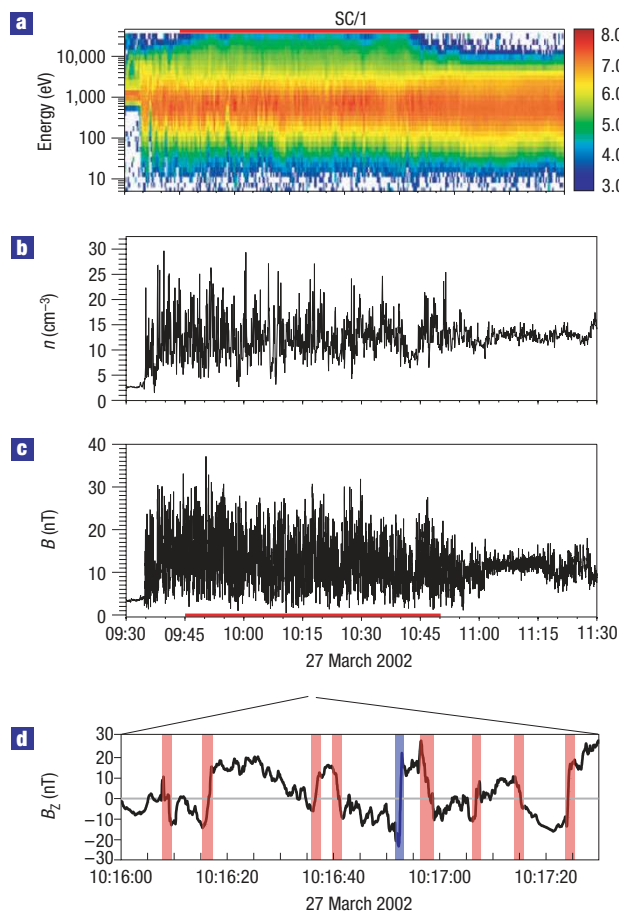
Figure 2 Overview of the quasi-parallel shock crossing. a, Spectrogram of the ion differential energy flux. **b**, Ion density, n. **c**, Magnitude of the magnetic field, B. **d**, Zoom-in of the B_Z component of the magnetic field in the time interval 10:16:00–10:17:30. The B_Z component of the magnetic field is the component exhibiting the largest changes and it is expressed in the GSE coordinate system shown in Fig. 1a. The zero level in **d** is indicated by a grey horizontal line. The thin current sheets are observed in the time interval 09:45–10:50 indicated by the red horizontal bars. In this region, strong fluctuations in density and magnetic field and accelerated and heated ions are observed.

Figure 3 Four-spacecraft SC/1 to SC/4 magnetic-field observations of the thin current sheet. a, Reconnecting component, B_L. **b**, Out-of-plane component, B_M. **c**, Normal component, B_N. **d**, Magnitude of the magnetic field, B. The different colours indicate different spacecraft. The zero level in **a–c** is indicated by a grey horizontal line. The magnetic-field components are plotted in the current-sheet coordinate system NML described in Fig. 1b. $\mathbf{L} = [0.36\ 0.12\ 0.94]$ GSE is the direction of maximum variance of the magnetic field. The time delays between the current-sheet crossings give $\mathbf{V}_{cs} \approx -200\ \mathbf{N}\ \mathrm{km\ s}^{-1}$, where $\mathbf{N} = [0.94\ 0.11\ -0.39]$ GSE is the normal direction to the current sheet. $\mathbf{M} = \mathbf{L} \times \mathbf{N}$ is the direction out-of-plane in Fig. 1b. The time series have been shifted with respect to SC/1 using the time delays between spacecraft so that the observations are in the current-sheet frame.

magnetic field and the normal to the shock is $10° < \theta < 30°$. This highly turbulent region is characterized by substantial ion heating and acceleration, Fig. 2a, together with strong fluctuations both in the density, Fig. 2b, and in the magnitude of the magnetic field, Fig. 2c. The detailed properties of the turbulence for this region will be discussed in a separate publication (D.S., A.R., A.V. and S. D. Bale, manuscript in preparation). Around 11:00, the shock changes from quasi-parallel to quasi-perpendicular ($\theta > 50°$), the fluctuations in density and magnetic field become smaller and the high-energy ions ($>10\ \mathrm{keV}$) disappear. Many thin current sheets with a typical width of a few ion inertial lengths, λ_i, are found in the magnetosheath downstream of the quasi-parallel shock during the time interval 09:45–10:50 but not downstream of the quasi-perpendicular shock. These observations indicate that the thin current sheets only form in the region with the strongest turbulence. As an example, Fig. 2d shows nine thin current sheets (colour shaded) over a 1.5 min interval. The current sheet around 10:16:52 (blue shaded) is analysed in detail in this paper to provide evidence of reconnection. Figure 3 shows
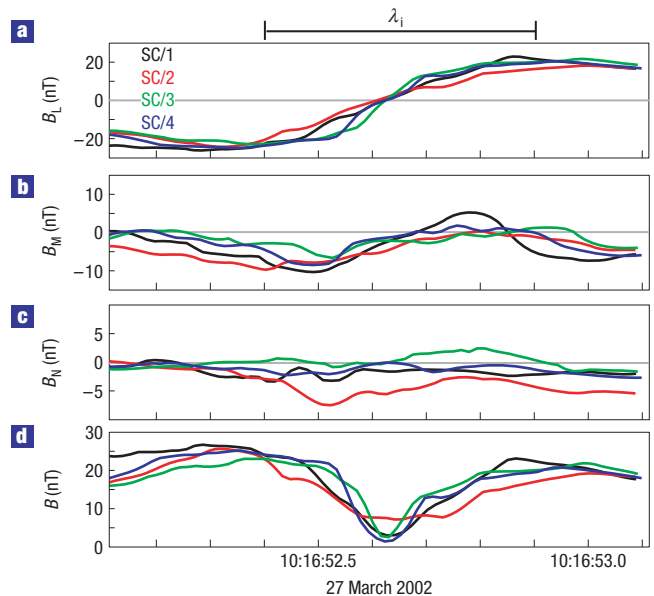
four-spacecraft magnetic-field observations of the current sheet around 10:16:52. The magnetic-field components are plotted in the local current-sheet coordinate system NML. This coordinate system is obtained by combining the minimum variance analysis[21] with multi-spacecraft timing[22] of the magnetic field under the assumption of a stationary and planar current sheet moving at constant velocity, V_{cs}, along its normal direction, $\mathbf{N}$. The multi-spacecraft timing gives $V_{cs} \approx 200\ \mathrm{km\ s}^{-1}$. The duration of the current-sheet crossing 10:16:52.4–52.9 is 0.5 s, which corresponds to a current-sheet thickness in the normal direction of about $100\ \mathrm{km} \approx 1\lambda_i$, obtained using V_{cs}. The four spacecraft all observe similar magnetic field during the current-sheet crossing, thus indicating that the current sheet is planar over the spacecraft separation $\sim\lambda_i$ and time stationary on a timescale of $\sim 1\ \mathrm{s}$, which is approximately one ion gyroperiod. Observations in Fig. 3 suggest that the spacecraft cross the current sheet during ongoing reconnection and very close to the X-line where reconnection is initiated, the so-called ion diffusion region. In the diffusion region, the electrons move together with the magnetic-field lines at the $\mathbf{E} \times \mathbf{B}/B^2$ velocity, whereas the ions do not, so that Hall magnetic field, B_M, and electric field, E_N, are created, as shown in the schematic diagram in Fig. 1b and expected from models and simulations[19,23,24] and from previous observations[7,8,25,26]. Figure 3b shows that, for all of the spacecraft, the out-of-plane component, B_M, has a bipolar signature consistent with Hall magnetic field, whereas the maximum variance component, B_L, reverses across the current sheet, Fig. 3a, and the magnitude of the magnetic field, B, has a deep minimum in the centre, Fig. 3d. B_N is slightly varying

but on average negative, Fig. 3c, as is expected during reconnection and discussed below.

To provide evidence of magnetic reconnection, Fig. 4 shows combined observations of density and electric and magnetic fields for spacecraft 4. Magnetic reconnection is ongoing when there is an electric field at the X-line locally tangential to it[23]. Thus, for a two-dimensional geometry such as the one in Fig. 1b, the strongest evidence of reconnection is an electric field in the out-of-plane direction, $E_{cs,M} < 0$, together with a normal magnetic field, $B_N \neq 0$. $E_{cs,M}$ is an absolute measure of the reconnection rate. The tangential electric field, $E_{cs,M}$, measured in the current-sheet reference frame, Fig. 4f, is varying but on average $E_{cs,M} \approx -0.5\,\mathrm{mV\,m^{-1}}$. The condition $E_{cs,M} < 0$ corresponds to plasma inflow towards the X-line from both sides of the current sheet at the velocity $V_{in} = V_{E \times B,N} = (\mathbf{E} \times \mathbf{B}/B^2)_N \simeq E_{cs,M}/B_L \simeq 25\,\mathrm{km\,s^{-1}}$ in the normal direction, see Fig. 4l where the vertical scale has been chosen so that this inflow can be clearly seen. In the centre of the current sheet, $V_{E \times B,N}$ becomes very large reaching values of up to $200–300\,\mathrm{km\,s^{-1}}$ (not shown). This is consistent with conservation of the magnetic flux transported across the current sheet (when B gets small $V_{E \times B,N}$ should increase) but it could also be due to a local enhancement of the reconnection rate or to the spacecraft crossing the electron diffusion region, Fig. 1b, where the electrons do not move with the $\mathbf{E} \times \mathbf{B}/B^2$ field-line velocity. We can estimate the dimensionless reconnection rate defined as $R = V_{in}/V_A$, where V_A is the Alfvén velocity on both sides of the current sheet. We find $R \approx 0.1$, implying that magnetic reconnection is fast, in agreement with numerical simulations[19] and previous observations[26]. $B_N \neq 0$ indicates that the two sides are magnetically connected, implying that the topology of the magnetic field has changed at the X-line. The normal magnetic field, Fig. 4c, is slightly varying but on average $B_N \approx -1\,\mathrm{nT}$.

During reconnection, electromagnetic energy is converted into kinetic and thermal energy of the plasma[1]. Thus, plasma acceleration away from the X-line and plasma heating also strongly substantiate ongoing reconnection. Figure 4i shows that $\mathbf{E} \cdot \mathbf{j} > 0$ within the current sheet and thus electromagnetic energy is converted into kinetic and thermal energy of the plasma, the average value $\mathbf{E} \cdot \mathbf{j} \approx 1\,\mathrm{nW\,m^{-3}}$. Electrons are accelerated away from the X-line at velocity $V_{E \times B,L}$ that is up to about $2V_A$, see Fig. 4j. Such velocities are expected from numerical simulations[19], which show that electrons and ions are respectively super-alfvenic and sub-alfvenic in the ion diffusion region, whereas away from it they move together at the Alfvén speed. Electron heating can be seen in Fig. 4m. The spectrogram of the differential energy flux, dEF, shows that the thermal energy of the electrons, which is approximately the energy corresponding to the maximum dEF, increases in the centre of the current sheet with respect to both sides.

The evidence of crossing the ion diffusion region is the observations of a bifurcated current sheet and of the Hall magnetic and electric fields, expected during symmetric reconnection[7,8,19,23–26]. The change in the reconnecting component, B_L (Fig. 4a), occurs in two main steps, thus indicating that the current sheet is bifurcated, as also seen in the out-of-plane current, j_M (Fig. 4h). The current shows two peaks at the edges of the current sheet consistent with the two peaks in the out-of-plane velocity of the electrons $V_{E \times B,M}$, see Fig. 4k. In the centre of the current sheet, j_M is not consistent with $-V_{E \times B,M}$ either because the j_M is mainly parallel to B there and the electron parallel velocity cannot be measured or because the spacecraft is crossing the electron diffusion region. B_M, Fig. 4b, has the typical Hall bipolar signature expected in the ion diffusion region. B, Fig. 4d, decreases in the centre of the current sheet down to very close to the magnetic null, $1.5\,\mathrm{nT}$, consistent with the spacecraft being close to the X-line in symmetric reconnection. The normal Hall
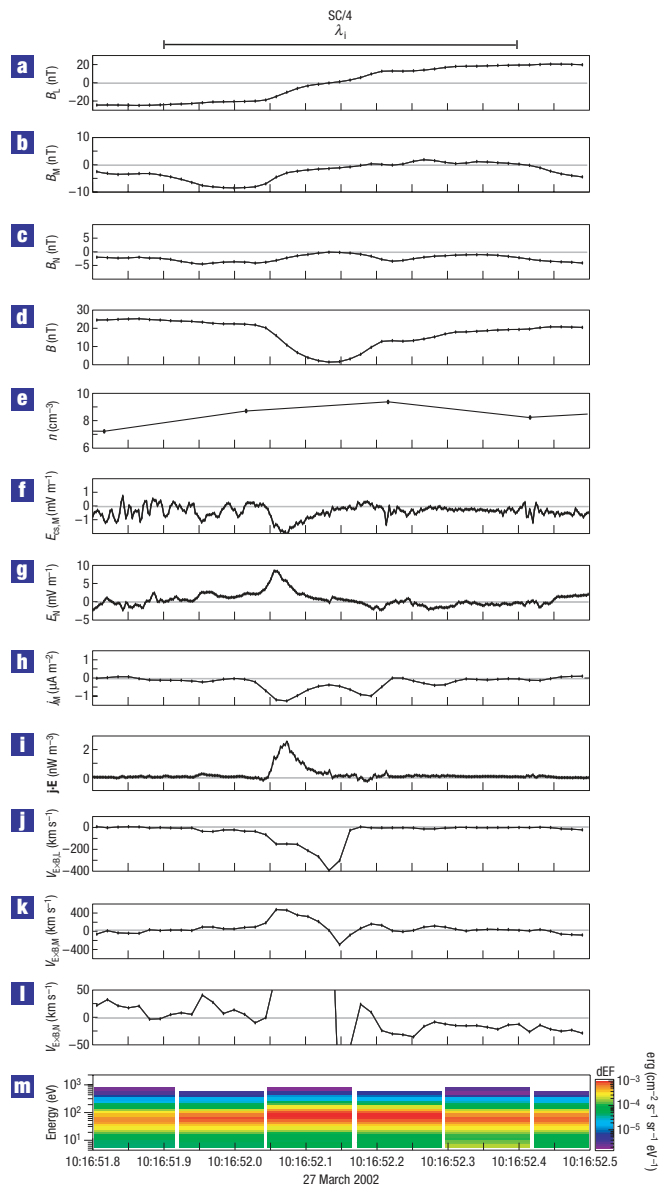

Figure 4 SC/4 high-resolution observations of the thin current sheet.
a, Reconnecting component, B_L. **b**, Out-of-plane component, B_M. **c**, Normal component, B_N. **d**, Magnitude of the magnetic field, B. **e**, Plasma density, n. **f**, Tangential electric field, $E_{cs,M}$, in the current-sheet frame. **g**, Normal electric field, E_N. **h**, Out-of-plane current, j_M, calculated from single-spacecraft magnetic-field measurements using Ampere's law. **i**, $\mathbf{E} \cdot \mathbf{j}$ in the current-sheet frame. **j**, L component of the $\mathbf{E} \times \mathbf{B}/B^2$ flow. **k**, M component of the $\mathbf{E} \times \mathbf{B}/B^2$ flow. **l**, N component of the $\mathbf{E} \times \mathbf{B}/B^2$ flow. **m**, Spectrogram of the electron differential energy flux, dEF. The spectrogram is obtained by integrating two-dimensional cuts of the electron distribution function measured every 120 ms. The velocity from the electron detectors cannot be used in this study because it is measured only every 4 s (the velocity calculations require the full three-dimensional distribution function). The zero level in each panel is indicated by a grey horizontal line. The components of E and B are plotted with different vertical scales. The two sides of the current sheet have approximately the same density and magnetic field. The plasma parameters on both sides of the current sheet are $n = 7\,\mathrm{cm^{-3}}$, $B = 25\,\mathrm{nT}$, ion temperature $T_i \simeq 200\,\mathrm{eV}$ and electron temperature $T_e = 50\,\mathrm{eV}$, which give ion inertial length $\lambda_i \simeq 90\,\mathrm{km}$, ion gyroradius $\rho_i \simeq 80\,\mathrm{km}$, Alfvén velocity $V_A \simeq 200\,\mathrm{km\,s^{-1}}$ and $\beta \simeq 1$. The ion and electron temperatures are measured by particle detectors. The duration of the current-sheet crossing 10:16:51.9–52.4 is 0.5 s corresponding to a current-sheet thickness $\approx 1\lambda_i$.

electric field, E_N (Fig. 4g), points on both sides towards the centre of the current sheet. There is a slight asymmetry between the two sides of the current sheet, E_N is stronger (up to $8\,\mathrm{mV\,m^{-1}}$) on the left side (in addition, the B_M component is stronger there). The electric potential drop across E_N on the left side of the current sheet (calculated between 16:51:95 and 16:52:15) is about ~100 V. A proton accelerated through such a potential jump gets a velocity ~$150\,\mathrm{km\,s^{-1}} \approx V_A$, that is, the expected velocity for ions outflowing away from the X-line. The observations are consistent with a crossing of the diffusion region south of the X-line as shown in Fig. 1b, namely $B_N < 0$, the sign of the bipolar B_M and $V_{E\times B,L} < 0$.

The observations in Fig. 4 together with multi-spacecraft observations in Fig. 3 provide evidence that the Cluster spacecraft are crossing the ion diffusion region during ongoing magnetic reconnection. The strongest evidence that reconnection is ongoing comes from the measurements of tangential electric field, normal magnetic field, plasma flows and thermal energy of the electrons, which show the plasma inflow and outflow in the reconnection region, the magnetic connection between both sides of the current sheet and the plasma heating during reconnection. The evidence for crossing the ion diffusion region is the Hall magnetic and electric fields. These results, combined with the fact that the reconnecting current sheet is found in the turbulent terrestrial magnetosheath, show, for the first time, *in situ* evidence of magnetic reconnection in a turbulent plasma. We clearly show that reconnection acts as an electromagnetic energy conversion mechanism as $\mathbf{E} \cdot \mathbf{j} > 0$, in particular we prove that electromagnetic energy is dissipated into heating of the turbulent plasma because the thermal energy of the electrons is increased. We also show that magnetic reconnection in turbulent plasma is fast. Our findings have important implications for laboratory and astrophysical plasmas, where magnetic reconnection and turbulence are ubiquitous and turbulent reconnection should be common.

Finally, we discuss the possible relevance of turbulent reconnection in generating high-energy ions and electrons, which is suggested by the observation of high-energy ions ($>10\,\mathrm{keV} \approx 50\,k_B T_i$) in Fig. 2a. *In situ* observations[27] indicate the absence of high-energy ions and electrons in the solar wind, where reconnection creates large-scale reconnection X-lines. However, high-energy electrons have been found in the terrestrial magnetotail[28], where reconnection is often localized within many small-scale magnetic islands. This is also indicated by numerical simulations[29,30]. We speculate that in a turbulent plasma, magnetic reconnection does not develop large-scale X-lines such as those at the terrestrial magnetopause[31] or in the solar wind[5], but instead it is most likely localized. If the production of high-energy particles occurs during localized small-scale reconnection, then particle acceleration to high energies should be common during turbulent reconnection. This can have important implications for particle acceleration in astrophysical plasmas, for example, for cosmic-ray acceleration[10]. However, to quantitatively assess particle acceleration due to turbulent reconnection, particle detectors with higher sensitivity and time resolution than those onboard Cluster are needed, such as those planned onboard the future mission NASA/MMS.

References

1. Priest, E. & Forbes, T. *Magnetic Reconnection* (Cambridge Univ. Press, Cambridge, 2000).
2. Aschwanden, M. J. *Physics of the Solar Corona: An Introduction* (Springer, Berlin, 2004).
3. Lin, J. *et al.* Direct observations of the magnetic reconnection site of an eruption on 2003 November 18. *Astrophys. J.* **622**, 1251–1264 (2005).
4. Gosling, J. T., Skoug, R. M., McComas, D. J. & Smith, C. W. Direct evidence for magnetic reconnection in the solar wind near 1 AU. *J. Geophys. Res.* **110**, 1107–1115 (2005).
5. Phan, T. D. *et al.* A magnetic reconnection X-line extending more than 390 Earth radii in the solar wind. *Nature* **439**, 175–178 (2006).
6. Paschmann, G. *et al.* Plasma acceleration at the earth's magnetopause —Evidence for reconnection. *Nature* **282**, 243–246 (1979).
7. Øieroset, M., Phan, T. D., Fujimoto, M., Lin, R. P. & Lepping, R. P. *In situ* detection of collisionless reconnection in the Earth's magnetotail. *Nature* **412**, 414–417 (2001).
8. Ren, Y. *et al.* Experimental verification of the Hall effect during magnetic reconnection in a laboratory plasma. *Phys. Rev. Lett.* **95**, 055003 (2005).
9. Tajima, T. & Shibata, K. (eds) *Plasma Astrophysics* (Addison-Wesley, Reading, 1997).
10. Kronberg, P. P., Colgate, S. A., Li, H. & Dufton, Q. W. Giant radio galaxies and cosmic-ray acceleration. *Appl. J. Lett.* **604**, L77–L80 (2004).
11. Simon, G. W., Title, A. M. & Weiss, N. O. Sustaining the Sun's magnetic network with emerging bipoles. *Astrophys. J.* **561**, 427–434 (2001).
12. Cothran, C. D., Landreman, M., Brown, M. R. & Matthaeus, W. H. Three-dimensional structure of magnetic reconnection in a laboratory plasma. *Geophys. Res. Lett.* **30**, 17–20 (2003).
13. Matthaeus, W. H. & Montgomery, D. *International Conf. on Nonlinear Dynamics* 203–222 (Annals New York Acad. Sci., Vol. 357, New York Acad. Sci., New York, 1980).
14. Matthaeus, W. H. & Lamkin, S. L. Turbulent magnetic reconnection. *Phys. Fluids* **29**, 2513–2534 (1986).
15. Carbone, V., Veltri, P. & Mangeney, A. Coherent structure formation and magnetic field line reconnection in magnetohydrodynamic turbulence. *Phys. Fluids* **2**, 1487–1496 (1990).
16. Dmitruk, P. & Matthaeus, W. H. Structure of the electromagnetic field in three-dimensional Hall magnetohydrodynamic turbulence. *Phys. Plasmas* **13**, 042307–042314 (2006).
17. Baumjohann, W. & Treumann, R. A. *Basic Space Plasma Physics* (Imperial College Press, London, 1996).
18. Burgess, D. *et al.* Quasi-parallel shock structure and processes. *Space Sci. Rev.* **118**, 205–222 (2005).
19. Pritchett, P. L. Collisionless magnetic reconnection in a three-dimensional open system. *J. Geophys. Res.* **106**, 25961–25978 (2001).
20. Escoubet, C. P., Schmidt, R. & Goldstein, M. L. Cluster—science and mission overview. *Space Sci. Rev.* **79**, 11–32 (1997).
21. Sonnerup, B. U. O. & Cahill, L. J. Jr. Magnetopause structure and attitude from Explorer 12 observations. *J. Geophys. Res.* **72**, 171–183 (1967).
22. Schwartz, S. J. *Analysis Methods for Multi-Spacecraft Data* 249–270 (ESA Publ. Div., Paris, 1998).
23. Sonnerup, B. U. O. *Solar System Plasma Physics* Vol. 3, 45–118 (North-Holland, Amsterdam, 1979).
24. Mandt, M. E., Denton, R. E. & Drake, J. F. Transition to whistler mediated magnetic reconnection. *Geophys. Res. Lett.* **21**, 73–76 (1994).
25. Mozer, F. S., Bale, S. D. & Phan, T. D. Evidence of diffusion regions at a subsolar magnetopause crossing. *Phys. Rev. Lett.* **89**, 015002 (2002).
26. Vaivads, A. *et al.* Structure of the magnetic reconnection diffusion region from four-spacecraft observations. *Phys. Rev. Lett.* **93**, 105001 (2004).
27. Gosling, J. T., Skoug, R. M., Haggerty, D. K. & McComas, D. J. Absence of energetic particle effects associated with magnetic reconnection exhausts in the solar wind. *Geophys. Res. Lett.* **32**, 14113–14117 (2005).
28. Øieroset, M., Lin, R. P., Phan, T. D., Larson, D. E. & Bale, S. D. Evidence for electron acceleration up to ~300 keV in the magnetic reconnection diffusion region of Earth's magnetotail. *Phys. Rev. Lett.* **89**, 195001 (2002).
29. Matthaeus, W. H., Ambrosiano, J. J. & Goldstein, M. L. Particle-acceleration by turbulent magnetohydrodynamic reconnection. *Phys. Rev. Lett.* **53**, 1449–1452 (1984).
30. Drake, J. F., Swisdak, M., Che, H. & Shay, M. A. Electron acceleration from contracting magnetic islands during reconnection. *Nature* **443**, 553–556 (2006).
31. Phan, T. D. *et al.* Extended magnetic reconnection at the earth's magnetopause from detection of bi-directional jets. *Nature* **404**, 848–850 (2000).